Improving the Channeler Ant Model for lung CT analysis

Piergiorgio Cerello[a], Ernesto Lopez Torres[b], Elisa Fiorina[c,a], Chiara Oppedisano[a], Cristiana Peroni[c,a], Raul Arteche Diaz[b], Roberto Bellotti[d,e], Paolo Bosco[f,g], Niccolò Camarlinghi[h,i], Andrea Massafra[j,k]

[a] Istituto Nazionale di Fisica Nucleare, Sezione di Torino, Via Giuria 1, I-10125, Torino;
[b]CEADEN, Calle 30 #502 e/ 5ta y 7ma Avenida, Playa, Ciudad Havana, Cuba;
[c]Dipartimento di Fisica Sperimentale, Università di Torino, Via Giuria 1, I-10125, Torino;
[d] Dipartimento Interateneo di Fisica, Università di Bari, Via Amendola 173, I-70126, Bari;
[e]Istituto Nazionale di Fisica Nucleare, Sezione di Bari, Via Amendola 173, I-70126, Bari;
[f] Dipartimento di Fisica, Università di Genova, Via Dodecaneso 33, I-16146,Genova;
[g]Istituto Nazionale di Fisica Nucleare, Sezione di Genova, Via Dodecaneso 33, I-16146, Genova;
[h]Dipartimento di Fisica, Università di Pisa, Largo Pontecorvo 3, I-56127 Pisa;
[i]Istituto Nazionale di Fisica Nucleare, Sezione di Pisa, Largo Pontecorvo 3, I-56127, Pisa;
[j]Dipartimento di Fisica, Università del Salento, via per Arnesano, I-73100, Lecce;
[k]Istituto Nazionale di Fisica Nucleare, Sezione di Lecce, via per Arnesano, I-73100, Lecce.

ABSTRACT

The Channeler Ant Model (CAM) is an algorithm based on virtual ant colonies, conceived for the segmentation of complex structures with different shapes and intensity in a 3D environment. It exploits the natural capabilities of virtual ant colonies to modify the environment and communicate with each other by pheromone deposition. When applied to lung CTs, the CAM can be turned into a Computer Aided Detection (CAD) method for the identification of pulmonary nodules and the support to radiologists in the identification of early-stage pathological objects. The CAM has been validated with the segmentation of 3D artificial objects and it has already been successfully applied to the lung nodules detection in Computed Tomography images within the ANODE09 challenge. The model improvements for the segmentation of nodules attached to the pleura and to the vessel tree are discussed, as well as a method to enhance the detection of low-intensity nodules. The results on five datasets annotated with different criteria show that the analytical modules (i.e. up to the filtering stage) provide a sensitivity in the $80 - 90\%$ range with a number of FP/scan of the order of 20. The classification module, although not yet optimised, keeps the sensitivity in the $70 - 85\%$ range at about 10 FP/scan, in spite of the fact that the annotation criteria for the training and the validation samples are different.

Keywords: Virtual Ants, CAD, lung CT

1. INTRODUCTION

Lung cancer, the most common cause of cancer-related deaths (about 28% and 19% of all cancer-related deaths in the United States and in the European Union, respectively), commonly manifests itself as non-calcified pulmonary nodules. Computed Tomography (CT), the most sensitive imaging modality for the detection of pulmonary nodules, is a promising approach for the detection of early-stage lung cancers in screening programs based on low-dose CT and for the reduction of the number of lung cancer deaths, as recently confirmed by the U.S. National Cancer Institute in its release of early results from the National Lung Screening Trial (NLST).[1] Since a large number of nodules (20 35%) can be missed in screening diagnoses[2] and the annotation time for a high resolution CT is quite long, Computer Aided Detection (CAD) methods could be very useful in supporting radiologists in the identification of early-stage pathological objects.

Further author information: (Send correspondence to Piergiorgio Cerello: E-mail: cerello@to.infn.it, Telephone: +39 011 6707046)

The Channeler Ant Model (CAM)[3] is developed by the MAGIC-5 Collaboration[4] as part of a multi-thread Computer Aided Detection (CAD) system for radiologist support in the lung cancer diagnosis, that also includes algorithms based on region growing[5] and Voxel-Based Neural Analysis.[6,7] Swarm Intelligence is the feature of a system whose collective behaviour produces the rising of patterns characteristic of the system. Each agent has limited knowledge and capabilities, doesn't know the global state of the system and interacts with other agents by modifying the environment through the deposition of pheromones. The CAM is an algorithm based on virtual ant colonies,[8,9] conceived for the segmentation of complex structures with different shapes and intensity in a 3D environment. It exploits the natural capabilities of virtual ant colonies to modify the environment and communicate with each other by pheromone deposition. The CAM has been validated with the segmentation of 3D artificial objects and it has already been successfully applied to the lung nodules detection in Computed Tomography images within the ANODE09 challenge,[10] showing that it can significantly contribute to the global performance of a multi-thread lung CAD system. The present work addresses its performance as a standalone module, with the evaluation of its performance on heterogeneous datasets with different annotation criteria.

2. THE CHANNELER ANT MODEL

The CAM extends to a 3D environment the basic concepts already applied to ant colonies and defines a set of rules that self-regulate the colony evolution, based on the implementation of the ant movement, the pheromone deposition and the life cycle: thanks to the introduction of a life parameter called energy, death and reproduction take place. The correlation between the pheromone deposition and the image intensity can be defined according to the goal of a specific deployment: therefore, the CAM can be used to analyse different images and to look for different structures, such as gray matter in brain MR images.[11] The analysis of artificial objects defines the CAM performance as a function of the object shape, the image dynamic range and noise and with respect to other segmentation models like region growing.[3] Any ant colony starts its evolution from an anthill set in a voxel that belongs to the object to be segmented and evolves according to the model rules until its extinction, leaving a pheromone map which is then analysed to study the properties of the segmented object. In order to segment relevant nodules in lung Computed Tomographies the CAM is deployed as the most important part of a sequence of four functional modules: lung segmentation, nodule hunter, filtering stage and neural network classification. The CAM provides the nodule hunting functionality as well as the basic information used for the filtering of CAD findings and the evaluation of the input features for the classification stage.

3. DATASETS

The present analysis was carried out on 5 different datasets, as shown in Table 1 : two sets of 69 CTs each from the LIDC database,[12] two sets of 40 and 20 CTs from the ITALUNG_CT screening project[13] and one set of 5 CTs from the ANODE09 study.[14] The number of relevant nodules for each subset is shown in Table 1: out of a total of 415, 138 were used for the cross-validation training and testing, 277 for the validation.

Table 1. Number of scans and of relevant nodules for the analysed datasets.

Dataset Name	Number of CTs	Number of relevant nodules
LIDC (train)	69	138
LIDC (validation)	69	113
ANODE09	5	39
ITALUNG_CT (1)	20	39
ITALUNG_CT (2)	41	86

Since the annotation criteria for the different datasets are not homogeneous, it must be taken into account that the comparison of the performances is subject to that intrinsic uncertainty. However, that is a real-life condition for any algorithm to be used by different radiolgists in different conditions. It is likely, anyway, that if the CAM use were restricted to a study with a common protocol for the nodule annotation (e.g., only nodules

with a radius larger than X mm), the performance could be further improved with a dedicated optimisation of the filtering criteria.

The gold standard for the comaprison of the CAM findings with the radiological findings was defined as follows:

- for the LIDC database, nodules annotated by at least 2 (out of 4) radiologists;
- for the ANODE09 and ITALUNG_CT databases, nodules declared as relevant.

Nodules identified by one radiologist in the LIDC dataset and declared as *not relevant* in the ANODE09 and ITALUNG_CT annotations were not considered, neither as true nor as false findings.

The matching condition between the radiological and the CAM findings was defined by the logical AND of the following conditions:

- the distance between the CAM and the radiological finding center is smaller then 1.5 times the radiological finding radius (the same condition used in[10]);
- at least 1 voxel in the CAM finding list is also part of the radiological finding, provided as a sphere in the ANODE09 and ITALUNG_CT and as a list of voxels in the LIDC datasets, respectively.

4. LUNG SEGMENTATION

The lung parenchyma in the CT is identified by means of a 3D region growing method and a wavefront algorithm for the definition of the lung surface on the inner side, followed by a morphological closing with a cylinder from the outside.[15] The *a posteriori* check on the training/testing and validation datasets confirmed that none of the radiological findings is rejected at this stage.

5. NODULE HUNTING

The CAM is iteratively deployed as a segmentation method for the vessel tree and the nodule candidates of the right and left lungs, separately.

The first ant colony segments the vessel tree, starting from an anthill in the vicinity of its root.

Ants live in the 3D environment identified by the lung volume provided by the segmentation stage and described in terms of positions and intensities of voxels.

The ant life cycle is a sequence of atomic time steps, during which they behave according to a predefined set of rules: they release pheromone while moving in the 3D environment; they change their energy, so as to reproduce or die depending on its value; they wander according to the moving rules.[3]

The voxel image intensities can be thought of as the amount of available food for the colony: therefore, voxel intensities should be progressively consumed when the number of visits increases. This mechanism, required to make the colony evolve and explore the environment, is implemented in a complementary way: whenever the limit to the maximum number of visits in a voxel is reached, the voxel is no more available as a destination. When all the ants in the colony have died, the process stops, the segmented object is removed from the original image and the coordinates of all the voxels that are part of the object are stored in a list.

In the remaining image, iteratively, any voxel with intensity above a predefined threshold (-700 H.U.) is a new anthill and a new ant colony is deployed from there and generates a pheromone image.

The procedure is repeated by trying as anthill each voxel in the lung volume with an intensity larger than the -700 H.U. threshold: when no more voxels meet the conditions to become anthills, the information provided by the global pheromone map is analyzed.

Fig. 1 and 2 show an example of a slice of a nodule identified by the radiologist(s) as seen in the original image and in the pheromone map in the central and the peripheral part, respectively. The central part is pretty similar, but on the peripheral image it is clear that the pheromone map is much cleaner than the original image.

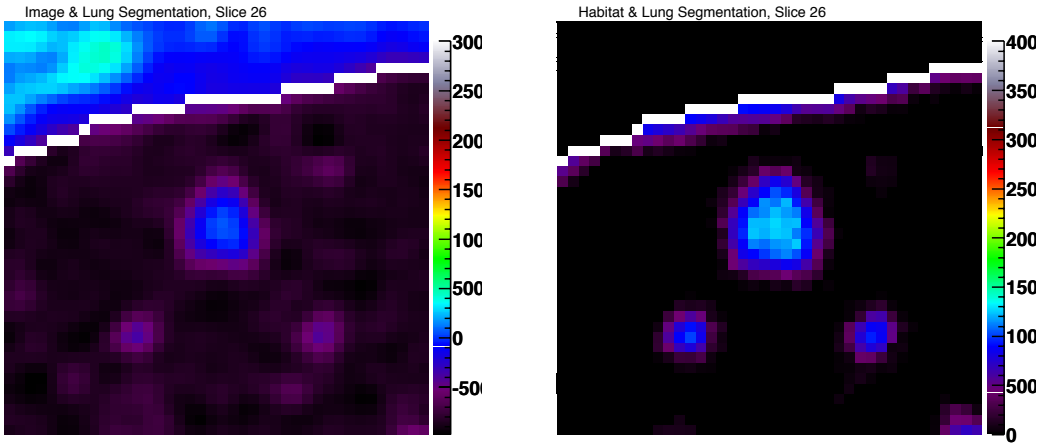

Figure 1. View of a central slice of a relevant nodule on the original image (left) and on the pheromone map (right).

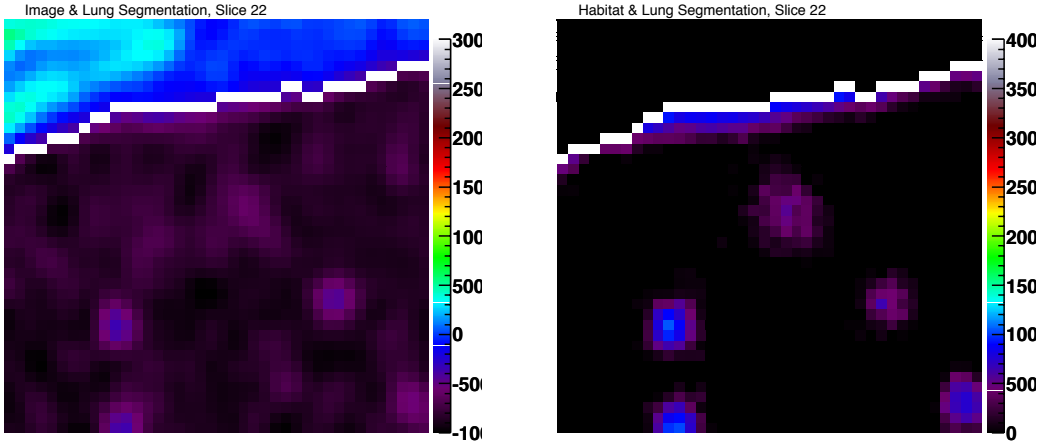

Figure 2. View of a peripheral slice of a relevant nodule on the original image (left) and on the pheromone map (right).

The pheromone map analysis is iterative: each voxel with a pheromone content above the minimum accepted value (8,000 units) is used as a seed for a region growing with an adaptive threshold. The threshold value is lowered iteratively for each seed and the selected value is the one corresponding to the minimum growth of the region when the hypothetical threshold is lowered by a quantum of 400 units.

Whenever a region is larger than a preset value (50 voxels, representing the minimum likely size of a structure that can contain a nodule as a sub-element), it is further analyzed in search of nodule candidates connected to it. In order to do so, a rolling sphere scans the finding and disentangles spherical-like structures. The procedure is repeated three times, with spheres of increasing initial radius (1.5, 2.5, 3.5 mm).

In short, a full sequence of ant colony deployments generates a pheromone release map that is analyzed by a dedicated module, which turns it into a list of candidate findings, each defined by a list of voxels and the values of a set of features related to their geometrical properties, their intensity pattern, their location in the lung.

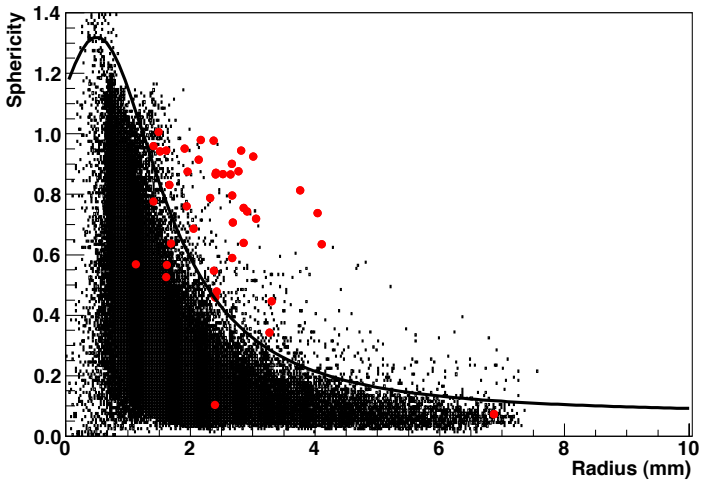

Figure 3. Correlation between the sphericity and the radius of the CAM findings for the ITALUNG_CT (2) dataset. The figure refers to the isolated findings, connected to the cage or not. The red dots represent the nodule candidates that match a radiological relevant findings. The black curve is the applied filtering function.

6. FILTERING

The number of candidates per CT, although depending on the number of slices, ranges between several hundreds to a few thousands per scan, a number far too large to be used as input for a neural network classifier. However, the vast majority of findings is easily rejected with some selections that make use of the correlation between some of the evaluated features: the radius, the sphericity, the fraction of voxels connected to the cage, the so called attach flag (AF), which identifies whether the finding is isolated (AF $= 0$) or not (AF > 0). If the finding is attached to a larger structure (i.e., the vessel tree), AF is related to the size of the rolling sphere and can range from 1 to 3.

The filtering is performed with a cut function on the histogram that correlates the sphericity to the radius (fig. 3): findings with a sphericity below the cut value at any given radius are rejected. Since the correlation between the radius and the sphericity depends on the AF value, for each AF value the function parameters are different. The filtering level is defined as a compromise between the requirement of maintaining a high sensitivity and the goal of forwarding as less as possible findings to the classification stage. An additional condition requires the fraction of voxels connected to the cage to be smaller than 0.65, in order to get rid of elongated artifacts attached to the cage.

7. MODEL IMPROVEMENTS

Among the limitations observed in the early deployments of the CAM on lung CTs,[10] two were particularly relevant to the global performance: the poor capability to identify nodules attached to large structures (the vessel tree or the pleura) and the difficult identification of small and low-intensity nodules.

The first problem was already discussed and it essentially involved a more sophisticated post-processing of the pheromone map, without changes to the CAM itself.

The second problem is related to the fact that for small low-intensity nodules the ant colony would extinguish too quickly to produce a pheromone image that could be identified by the region growing based pheromone map analysis. Since the pheromone deposition as a function of the image intensity is defined once and for all, the ant capability to explore low intensity voxels depends on the rate of its energy variation, i.e. on how many steps in low intensity voxels they can take before their energy decreases down to the death level. Furthermore, when objects are very small, the initial random movement can play an important role in causing the premature colony extinction.

The issue was addressed with a change in the ant colony evolution dynamic. However, the implementation had to take into account that a shift in the equilibrium between ant births and deaths could cause an exponential growth of the population and therefore a memory saturation. The ant energy parameters (the initial ant energy and the energy variation rate) are now set at the colony generation so as to cause a quicker ant reproduction. Only when the colony population grows above $1,000$ units, the parameters are reset to the model default values, so as to avoid that the colony population diverge: in such a way, a better pheromone image for small and low-intensity nodules is obtained without affecting the segmentation of large structures.

8. NEURAL NETWORK CLASSIFICATION

Until the end of the filtering stage, very few of the nodule candidate features are used. In particular, no direct information about the image intensities in the candidate voxels is taken into account.

The neural network classification, although not yet optimised, makes use of a selected set of features that are related to the finding size, shape, location, intensity (inside and on the border), as well as the above-defined AF value, which corresponds to different parameters of the nodule hunting algorithm and therefore to different ranges in the intensity and shape-related features.

The classification was carried on with a four layer feed-forward neural-network: 12 neurons in the input layer, 25 and 7 in the intermediate layers and - obviously - one in the output layer.

The full list of features for the input layer was the following: sphericity, radius, Shannon entropy of the inner and the border voxels, skewness, kurtosis, average and standard deviation of the inner and the border voxel intensities, fraction of voxels connected to the cage, AF value. The classification was optimized on the training/testing sample of 69 CTs and 138 true findings, with a cross validation procedure: 30 sub-list of true findings and false findings were classified as testing sample against all the other true and false findings used as training sample.

The parametrization of the neural network through the weights associated to the neuron connections was then used to classify the findings from the LIDC validation dataset and from the ANODE09 and ITALUNG_CT datasets.

9. RESULTS

Table 2 shows the relevant nodule statistics for the different datasets as well as the sensitivity and the average number of FP/scan after the filtering stage (i.e., at the beginning of the neural-network classification).

Table 2. Sensitivity and number of FP/scan before the classification stage for the analysed datasets.

Dataset Name	Sensitivity	FP/scan	Missed by CAM	Filtered
LIDC (train)	87.7% (121/138)	20.3	7	10
LIDC (validation)	79.6% (90/113)	19.9	10	13
ANODE09	76.9% (30/39)	10.4	4	5
ITALUNG_CT (1)	89.7% (35/39)	13.1	0	4
ITALUNG_CT (2)	80.2% (69/86)	21.6	3	14

The fraction of missed nodules ranges from 10 to 20%; about 2/3 of them (46) are lost in the filtering stage, the remaining 24 are not detected by the pheromone map analysis.

The performance, however, is similar for the different datasets, certainly within the uncertainty introduced by the differences in the annotation procedures. Some possible ways of improving the nodule segmentation have already been identified and will be investigated soon. In particular, it looks like the nodules identified without requiring the search for sub-structures are sometimes badly segmented, a feature that may be related to the nodule itself (isolated nodules are generally smaller than attached nodules) or to the algorithm. It is also

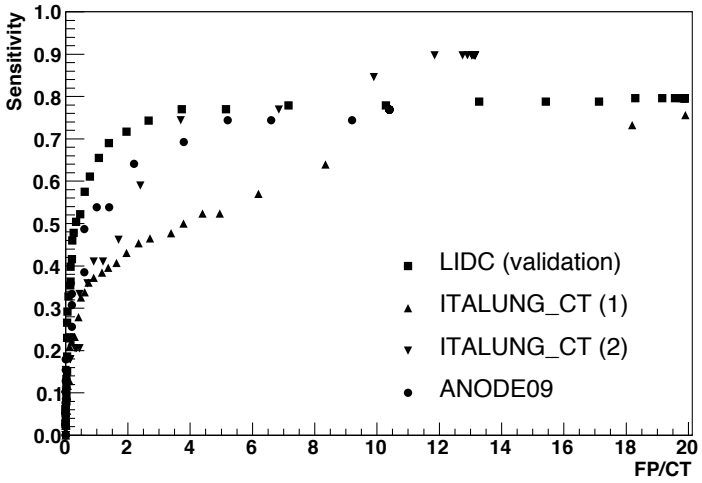

Figure 4. FROC curves for the validation datasets.

worth mentioning that the fraction of false findings attached to the lung cage as identified by the lung volume segmentation module is not far from 50%, as shown in Table 3. In other words, improving the lung segmentation module could provide as much benefit in terms of false findings reduction as a better nodule hunting and filtering.

Table 3. Fraction of false positive findings that are connected to the cage.

Dataset Name	FP connected to the lung cage (%)
LIDC (train)	57%
LIDC (validation)	49%
ANODE09	58%
ITALUNG_CT (1)	47%
ITALUNG_CT (2)	44%

The neural network was trained and tested on the 69 CTs of the LIDC database labeled as *LIDC (train)*, that include 138 relevant nodules. It has then been applied to the other datasets, with the results shown in fig. 4. Although there are significant differences in the performance, at about $10 - 12$ FP/scan, the sensitivity ranges between 70% and 85%. Taking into account the statistical uncertainty and the systematic error related to the different annotation procedure, the results are compatible and quite satisfactory. It must be remarked that the best result of the classification module is obtained for the LIDC validation sample, the one with the same annotation procedure used for the training sample.

10. CONCLUSIONS

The CAM presents some interesting features that make it worth exploring its performance in the analysis of lung CTs and medical images in general: it is a non-linear probabilistic approach that could in principle overcome some of the limitations of other methods (e.g., region growing). Early results showed that, even with a relatively poor performance, it was decisive in contributing to the improvement of results by other methods[10] . After addressing some of its limitations, the CAM is now performing much better and has become the leading contributor to the results of the MAGIC-5 multi-thread CAD, as recently shown in an analysis focused on the LIDC database.[16] The present work addresses the problem of implementing a global standalone algorithm general enough to provide an equivalent performance of lung CTs coming from different sources. The results show that it is possible to

obtain a satisfactory performance, with a sensitivity in the $70\% - 85\%$ range at about 10 FP/scan even when the annotation criteria for the training and the validation samples are not the same. The analysis of missing nodules and false findings shows that there is still room to improve the standalone CAM performance: the key step will be related to the inclusion of a calibration module that will evaluate and apply a global equalization to all the findings coming from a given CT.

11. ACKNOWLEDGMENTS

The authors wish to thank all the teams that hardly work to provide publicly available annotated databases.

REFERENCES

[1] Online document U.S. National Cancer Institute November 2010. *http://www.cancer.gov/clinicaltrials/noteworthy-trials/nlst*. Accessed 16 December 2010.

[2] Roberts HC, Patsios D, Kucharczyk DM, Paul N, and Roberts TP, The utility of computer-aided detection (CAD) for lung cancer screening using low-dose CT. *Computer Assisted Radiology and Surgery, Proceedings of the 19th International Congress and Exhibition*, Berlin, June 22 - 25, 2005, International Congress Series 1281, pp. 11371142.

[3] Cerello P, et al., 3-D object segmentation using ant colonies. *Pattern Recognition* 43 (4), 1476-1490, 2010.

[4] Bellotti R, et al., Distributed Medical Images Analysis on a Grid Infrastructure. in *Future Generation Computer Systems*, volume 23, pages 475-484, 2007.

[5] Bellotti R, et al., A CAD system for nodule detection in low-dose lung CTs based on Region Growing and a new Active Contour Model. *Medical Physics*, 34 (12), 4901-4910, 2007.

[6] Retico A, et al., Lung nodule detection in low-dose and thin-slice computed tomography. *Comput. Biol. Med.*, 38(4):525534, 2008.

[7] Retico A, et al., Pleural nodule identification in low-dose and thin-slice lung computed tomography. *Comput Biol Med.* 39(12):1137-1144, 2009.

[8] Ramos V., Fernandes C., and Rosa A.C. Self-regulated artificial ant colonies on digital image habitats. In *Proc. ICANN'05:* 15^{th} *Int. Conf.*, volume 3696, pages 311–316. Springer-Verlag LNCS Series, 2005.

[9] Khajehpour P., Lucas C., and Araabi B. Hierarchical image segmentation using ant colony and chemical computing approach. In *Advances in Natural Computation*, volume 3611, page 1250, Springer Verlag, 2005.

[10] Van Ginneken B. et al, Comparing and combining algorithms for computer-aided detection of pulmonary nodules in computed tomography scans: the ANODE09 study. *Medical Image Analysis* 14(6):707-722, 2010.

[11] Fiorina E, White matter segmentation in simulated MRI images using the Channeler Ant Model. *Proceedings of the 6th Internation Conference on Technology and Medical Sciences*, Porto, October 21 - 23, 2010.

[12] http://imaging.cancer.gov/programsandresources/InformationSystems/LIDC.

[13] Pegna A.L. et al., Design, recruitment and baseline results of the ITALUNG trial for lung cancer screening with low dose spiral CT. *Lung Cancer* 64 (1), 34-40, 2009.

[14] http://anode09.isi.uu.nl/, Automatic NOduleDEtection.

[15] De Nunzio G. et al., Automatic Lung Segmentation in CT Images with Accurate Handling of the Hilar Region. *Journal of Digital Imaging*, DOI: 10.1007/s10278-009-9229-1, 2010.

[16] Camarlinghi N. et al, Combination of Computer-Aided Detection algorithms for automatic lung nodule identification, submitted to *International Journal of Computer Assisted Radiology and Surgery*, 2010.